

Observation of ^8B Solar Neutrinos in the Kamiokande-II Detector

K. S. Hirata, T. Kajita, K. Kifune, K. Kihara, M. Nakahata, K. Nakamura, S. Ohara, Y. Oyama, N. Sato,
M. Takita, Y. Totsuka, and Y. Yaginuma

Institute for Cosmic Ray Research, University of Tokyo, Tanashi, Tokyo 188, Japan

M. Mori, A. Suzuki, K. Takahashi, T. Tanimori, and M. Yamada^(a)

National Laboratory for High Energy Physics (KEK), Tsukuba, Ibaraki 305, Japan

M. Koshiba

Tokai University, Shibuya, Tokyo 151, Japan

T. Suda

Department of Physics, Kobe University, Kobe, Hyogo 657, Japan

K. Miyano, H. Miyata, and H. Takei

Niigata University, Niigata, Niigata 950-21, Japan

K. Kaneyuki, Y. Nagashima, and Y. Suzuki^(b)

Department of Physics, Osaka University, Toyonaka, Osaka 560, Japan

E. W. Beier, L. R. Feldscher, E. D. Frank, W. Frati, S. B. Kim, A. K. Mann, F. M. Newcomer,
R. Van Berg, and W. Zhang

Department of Physics, University of Pennsylvania, Philadelphia, Pennsylvania 19104

(Received 10 April 1989)

Neutrinos from the decay of ^8B in the Sun have been observed in the Kamiokande-II detector. Based on 450 days of data in the time period January 1987 through May 1988, the measured flux obtained from data with $E_e \geq 9.3$ MeV is $0.46 \pm 0.13(\text{stat.}) \pm 0.08(\text{syst.})$ of the value predicted by the standard solar model. Within experimental errors, the Kamiokande-II value is in agreement with the corresponding value obtained in the ^{37}Cl radiochemical detector in essentially the same time period.

PACS numbers: 96.60.Kx, 95.85.Qx, 96.40.Qr

Our knowledge of the Sun is formulated in a quantitative description known as the standard solar model (SSM).¹ Central to that model is the assumption that the energy source of the Sun is nuclear fusion. The series of nuclear reactions in the various fusion chains involve the emission of electron-type neutrinos (ν_e) from several of the nuclear β -decay or electron-capture reactions,² the energies of the ν_e extending up to approximately 14 MeV. These neutrinos are of particular interest because, unlike the photons emitted by the Sun, they probe the interior of the Sun, and thereby are a sensitive test of the standard solar model. But, also, of special importance to elementary-particle physics, the solar neutrinos provide a means of studying the intrinsic properties of the neutrinos themselves because of the changing density³ and high magnetic field of the Sun,⁴ and the long Sun-Earth distance.⁵

The observation of solar neutrinos⁶ was initiated in about 1970, in a detector utilizing ^{37}Cl as the neutrino target. ^{37}Cl is especially sensitive to the 0.86-MeV ν_e from $e^- + ^7\text{Be} \rightarrow ^7\text{Li} + \nu_e$, and the 0-14-MeV continuous-spectrum ν_e from the two processes $p + ^7\text{Be} \rightarrow ^8\text{B} + \gamma$ and $^8\text{B} \rightarrow ^8\text{Be}^* + e^+ + \nu_e$. The average total

rate of ν_e interactions in the detector from 1970 to the end of 1985 was 2.1 ± 0.3 SNU,^{6,7} where a solar neutrino unit (SNU) is 10^{-36} interactions per target atom per second. The discrepancy between the value of 2.1 ± 0.3 SNU from the ^{37}Cl experiment and the value of 7.9 ± 2.6 (3σ) SNU predicted by the SSM² has persisted for more than a decade, and is often referred to as the solar neutrino puzzle.

In this Letter we report on the first observation in real time of the flux of ^8B solar neutrinos using the Kamiokande-II detector. Kamiokande-II is an imaging water Cherenkov detector which detects ^8B solar neutrinos by neutrino-electron scattering, $\nu_e e^- \rightarrow \nu_e e^-$, and yields information on the neutrino arrival time, the direction, and the energy spectrum.

The Kamiokande-II detector has been operating since the beginning of 1986. It is described in detail elsewhere.⁸ The detector volume containing 2140 tons of water is viewed by an array of 20-in.-diam photomultiplier tubes (PMT's) on a $1 \times 1\text{-m}^2$ lattice on the surface. The photocathode coverage amounts to 20% of the total inner surface. The attenuation length of the water for Cherenkov light averaged over the data-taking period is

48 m. The inner detector is completely surrounded by a water Cherenkov counter of thickness ≥ 1.4 m to ensure the containment of low-energy events. The outer counter also is an absorber of γ rays from the surrounding rock and a monitor of cosmic-ray muons.

The detector is triggered by at least 20 (18) hit PMT's within 100 nsec. The trigger accepts 7.6- (6.7-) MeV electrons with 50% efficiency and 10- (8.8-) MeV electrons with 90% efficiency over the fiducial volume of the detector. The numbers in the parentheses are the corresponding values after October 1987. Charge and time information for each channel above threshold is recorded for each trigger. The raw trigger rate is 0.6 (1.2) Hz of which 0.37 Hz is cosmic-ray muons. The remaining rate is due to radioactive contamination in the detector and external γ rays.

The energy calibration is performed with γ rays of energy up to 9 MeV from the reaction $\text{Ni}(n,\gamma)\text{Ni}$, with electrons from muon decays, and with the β decays from spallation products of cosmic-ray-muon interactions.⁹ From these calibrations, the absolute energy normalization is known to be better than 3%. The rms energy resolution for an electron is expressed by $22\%/[E_e/(10 \text{ MeV})]^{1/2}$. The rms angular resolution is 28° for an electron of 10 MeV. These numbers are obtained by Monte Carlo calculations, which reproduce well the calibration data of γ rays from the $\text{Ni}(n,\gamma)\text{Ni}$ reaction.

The search for ^8B solar neutrinos was carried out on the 450 days of data with relatively low radioactive background which were taken from January 1987 through May 1988. Events that satisfy the following three criteria were selected: (1) The total number of photoelectrons (PE) per event in the inner detector had to be less than 100, corresponding to a 30-MeV electron; (2) the total number of photoelectrons in the outer detector had to be less than 30, ensuring event containment; and (3) the time interval from the preceding event had to be longer than 100 μsec , to exclude electrons from muon decays.

The vertex positions and the directions of the selected events are reconstructed with an algorithm based on the time and position of hit PMT's. The rms vertex-position resolution is 1.7 m for 10-MeV electrons. Most of the γ rays which come from the rock have vertex positions near the wall of the detector, and are rejected by limiting the fiducial volume to 680 tons, which is 2 m inside the barrel and bottom PMT layers and 3.14 m inside the top PMT layer. The fiducial-volume cut reduces the event rate by an order of magnitude as shown in curves *a* and *b* in Fig. 1.

A number of remaining events are found to be due to unstable spallation products of throughgoing muons in the detector. These β -decay events have time and spatial correlation with the preceding cosmic-ray muons. Spallation products with long lifetime ($\tau_{1/2}=0.6\text{--}8$ sec) are observed, with likely assignment to ^8B , ^8Li , and ^{16}N , to-

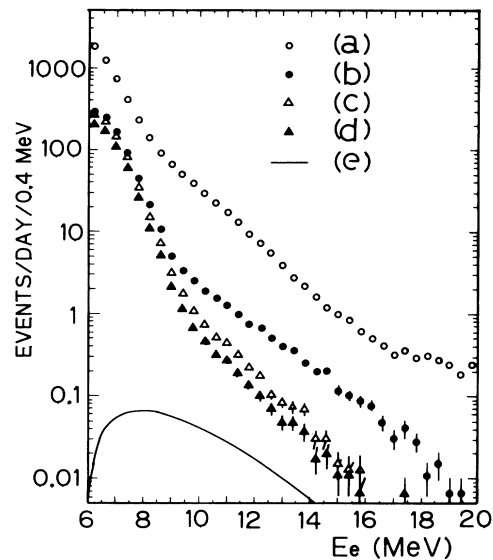


FIG. 1. Differential energy distribution of low-energy events: curve *a*, in the total mass of 2140 tons; *b*, in the fiducial mass of 680 tons; *c*, after the type-1 spallation cut; *d*, after the γ -ray cut. Curve *e*, Monte Carlo prediction of the standard solar model after all the cuts; the exact curve depends on the specific cuts applied.

gether with short-lifetime products ($\tau_{1/2}\sim 20$ msec), probably from ^{12}B and ^{12}N . The relative contribution from long- and short-lifetime products is approximately 0.55:0.45. To reduce events due to β decays from spallation-produced nuclei, two types of criteria were considered. In the first type, events are cut if they have a small time gap (ΔT) from and spatial correlation (ΔR) with the preceding muons, which are mostly accompanied by energetic showers. The pulse heights of these muon events are divided into the following three ranges:¹⁰ (1) 10000–20000 PE; (2) 20000–40000 PE; and (3) ≥ 20000 PE. Rejection criteria for ($\Delta T, \Delta R$) are for (1), (≤ 0.1 sec, ≤ 3 m); for (2), (≤ 3 sec, ≤ 3 m) and (3–15 sec, ≤ 2 m); for (3), (≤ 0.1 sec, no constraint on ΔR), (0.1–6 sec, ≤ 3 m), and (6–15 sec, ≤ 2 m). In addition, any event in the time interval of 30 sec following a muon which produced a spallation product is eliminated. In the second type, the requirement is imposed that the time of any low-energy event relative to the time of the previous cosmic-ray muon be greater than 100 msec; additionally, low-energy events are removed which occur within 40 sec of each other because of multiple β -decaying nuclei produced by a single interacting muon. The criteria of the first (second) type reduce the event sample with $E_e \geq 10$ MeV by 70% (51%), and introduce a dead time of 10.4% (3.2%); the efficiency to remove spallation events is about 90% (70%). In the following we present the results with the first type of spallation cut imposed.

The energy spectrum of the resultant events after the

spallation cut is given by curve *c* in Fig. 1. The spectrum consists of two components, arising from energetically "soft" and "hard" events. The soft component is due to radioactivity in the water, especially ^{214}Bi , a decay product of ^{222}Rn . The hard component is due to spallation products and to external γ rays which are not completely eliminated by the present cuts. To reduce the soft component we use only the data sample with $E_e \geq 9.3$ MeV in what follows.

To reduce the remaining γ rays in the region of the hard component of the background, events were also rejected which had vertex positions near the edge of the fiducial volume (outer 1-m layer) and directions inward (cosine of the angle relative to the normal to the nearest wall > 0.67). This " γ -ray" cut further reduced the event rate by $\sim 40\%$, and introduced an additional dead time of 13%. The event rate as a function of electron energy after this cut is also shown, as curve *d*, in Fig. 1. To test whether the γ -ray cut is biased by the directional criteria, the analysis was repeated with various smaller fiducial volumes without the γ -ray cut. Within statistics, the observed solar neutrino signals were the same as the corresponding result for the larger (680 tons) fiducial region with the γ -ray cut.

The event sample was then tested for a directional correlation with the Sun. This test provides an additional order-of-magnitude discrimination against the background rate of curve *d* in Fig. 1. Figure 2 shows the dis-

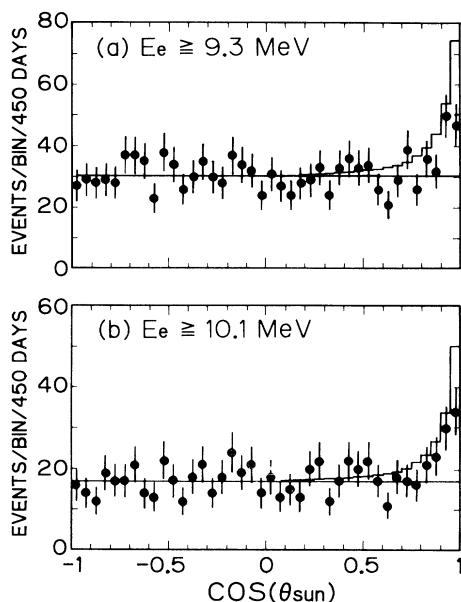


FIG. 2. Distributions in $\cos\theta_{\text{Sun}}$, the cosine of the angle between the trajectory of an electron and the direction of the Sun at a given time. The data are in the 680-ton fiducial region (a) with $E_e \geq 9.3$ MeV and (b) with $E_e \geq 10.1$ MeV, respectively. Events identified as spallation products or remaining γ rays have been excluded.

tribution in $\cos\theta_{\text{Sun}}$ for $E_e > 9.3$ MeV and $E_e > 10.1$ MeV, in which $\cos\theta_{\text{Sun}} = 1$ corresponds to the expected direction to the Earth from the Sun. A clear enhancement around $\cos\theta_{\text{Sun}} = 1$ with an isotropic background is evident. The solid histogram in the figure gives the signal expected from a Monte Carlo simulation based on the SSM.² The analysis was repeated with the detector location assigned to other, incorrect, latitudes and longitudes. The signal peaks only when the true Kamiokande coordinates are assigned.

Two independent analyses were performed on the same data. Each analysis obtained the final sample using totally independent programs for the event reconstruction and applied different cuts (see, for example, the description of two types of spallation cuts above). The results of the two analyses were carefully compared in many ways after each cut. The agreement on the measured signal between the two analyses is within the experimental errors.

To obtain the energy distribution of the solar neutrino signal, a fit of the $\cos\theta_{\text{Sun}}$ distribution with a flat background plus an expected angular distribution of the signal was performed for each energy bin. The resulting E_e spectrum is shown in Fig. 3, where it is compared with the corresponding spectrum predicted by the standard solar model.

The measured value of the ^8B solar neutrino flux for $E_e \geq 9.3$ MeV from the Kamiokande-II detector in the time period January 1987 through May 1988 (450 live detector days) is given by

$$\frac{\text{Kam-II data}}{\text{SSM}} = 0.46 \pm 0.13(\text{stat.}) \pm 0.08(\text{syst.}), \quad (1)$$

where SSM is the central value predicted by a Monte Carlo calculation based on the standard solar model² and subject to the same event criteria and experimental resolution as the data. Only the relative result is given in Eq. (1) because the flux below $E_e \leq 9.3$ MeV is not determined in this observation. The systematic error of

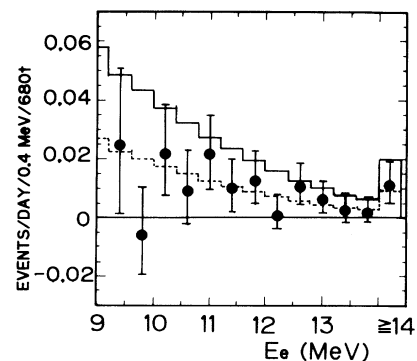


FIG. 3. Energy distribution of the solar neutrino signal (see text). The histogram is the distribution predicted by the SSM. The highest bin corresponds to $E_e \geq 14$ MeV. The dotted line shows the best fit to the data (0.46 SSM).

the measured flux is mainly due to the uncertainties in energy calibration ($\pm 3\%$) and in angular resolution ($\pm 4^\circ$).

The result in Eq. (1) may be compared with that obtained by the ^{37}Cl detector, 4.2 ± 0.8 SNU, in essentially the same time interval.⁷ Two limiting cases may be considered as responsible for any discrepancy between the ^{37}Cl data and the SSM. (i) In one limit, all contributions to the total flux observed by and predicted for the ^{37}Cl detector may be reduced, and (ii) in the other limit, a suppression of ^8B solar neutrino flux alone may cause the discrepancy. For the ^8B solar neutrino flux, one finds in case (i) $^{37}\text{Cl data/SSM} \approx (4.2 \pm 0.8)/7.9 = 0.53 \pm 0.1$, and for case (ii) $^{37}\text{Cl data/SSM} \approx [(4.2 \pm 0.8) - 1.8]/(7.9 - 1.8) = 0.39 \pm 0.1$, where 1.8 SNU is the expected rate due to nuclear processes other than ^8B .² Accordingly,

$$0.39 \pm 0.1 \leq \frac{^{37}\text{Cl data}(^8\text{B})}{\text{SSM}(^8\text{B})} \leq 0.53 \pm 0.1.$$

Thus, the result from the ^{37}Cl detector is consistent with the Kam-II value in Eq. (1) within the errors of the two measurements.

In conclusion, the ^8B solar neutrino flux measured by Kamiokande-II is $0.46 \pm 0.13(\text{stat.}) \pm 0.08(\text{sys.})$ of the value predicted by the standard solar model. This result is consistent with the value obtained by the ^{37}Cl experiment in essentially the same time period.

We gratefully acknowledge the cooperation of the Kamioka Mining and Smelting Company. We thank K. Arisaka and B. G. Cortez for their contributions to the early stage of this experiment. This work was supported by the Japanese Ministry of Education, Science and Culture, by the U.S. Department of Energy, and by the University of Pennsylvania Research Fund. Part of the analysis is carried out on FACOM M780 and M380 at the computer facilities of the Institute for Nuclear Study, University of Tokyo.

^(a)On leave from Niigata University, Niigata, Niigata 950-21, Japan.

^(b)Present address: Institute for Cosmic Ray Research, University of Tokyo, Tokyo, Japan.

¹See, for example, D. D. Clayton, *Principles of Stellar Evolution and Nucleosynthesis* (MacGraw-Hill, New York, 1968).

²J. N. Bahcall and R. K. Ulrich, *Rev. Mod. Phys.* **60**, 297 (1988), and references therein.

³L. Wolfenstein, *Phys. Rev. D* **17**, 2369 (1978); S. P. Mikheyev and A. Yu. Smirnov, *Nuovo Cimento* **9C**, 17 (1986); H. A. Bethe, *Phys. Rev. Lett.* **56**, 1305 (1986).

⁴M. B. Voloshin, M. I. Vysotskii, and L. B. Okun, *Yad. Fiz.* **44**, 677 (1986) [*Sov. J. Nucl. Phys.* **44**, 440 (1986)]; M. B. Voloshin and M. I. Vysotskii, *Yad. Fiz.* **44**, 845 (1986) [*Sov. J. Nucl. Phys.* **44**, 544 (1986)].

⁵S. M. Bilenky and B. Pontecorvo, *Phys. Rep.* **41**, 225 (1978); V. Gribov and B. Pontecorvo, *Phys. Lett.* **28B**, 493 (1969).

⁶J. K. Rowley, B. T. Cleveland, and R. Davis, Jr., in *Proceedings of a Conference on Solar Neutrinos and Neutrino Astronomy*, edited by M. L. Cherry, K. Lande, and W. A. Fowler, AIP Conference Proceedings No. 126 (American Institute of Physics, New York, 1985), p. 1; R. Davis, Jr., in *Proceedings of the Seventh Workshop on Grand Unification, ICOBAN '86*, edited by J. Arafune (World Scientific, Singapore, 1987), p. 237.

⁷The rate from October 1986 to May 1988 is reported to be 4.2 ± 0.8 SNU, according to R. Davis, Jr., in *Proceedings of the Thirteenth International Conference on Neutrino Physics and Astrophysics, Neutrino '88*, edited by J. Schneps *et al.* (World Scientific, Singapore, to be published).

⁸K. S. Hirata *et al.*, *Phys. Rev. D* **38**, 448 (1988).

⁹M. Nakahata, Ph.D. thesis, University of Tokyo Report No. UT-ICEPP-88-01, 1988 (unpublished); K. Hirata *et al.*, in *The Standard Model, The Supernova 1987A*, edited by J. Tran Thanh Van, *Proceedings of the Twenty-Second Rencontres de Moriond, Les Arcs, France, 1987* (Editions Frontiers, Gif-sur-Yvette, 1987), p. 689.

¹⁰A typical throughgoing muon gives a total pulse height of ~ 12000 PE, or approximately 3.4 PE/MeV. The muon rates in each range are (1) 0.16, (2) 2.8×10^{-2} , and (3) 8.0×10^{-3} , all in Hz.